PASSIVITY BASED NONLINEAR ATTITUDE CONTROL OF THE RØMER SATELLITE

Michael Melholt Quottrup, Jakob Krogh-Sørensen, and Rafał Wiśniewski

Aalborg University, Institute of Electronic Systems, Department of Control Engineering,
Fredrik Bajers Vej 7C, 9220 Aalborg Ø, Denmark.

October 2000

This paper suggests nonlinear attitude control of the Danish satellite Rømer. This satellite will be designed to fulfil two scientific objectives: The observation of stellar oscillations and the detection and localisation of gamma-ray bursts. The satellite will be equipped with a tetrahedron configuration of Wide Angle Telescopes for Cosmic Hard x-rays (WATCH), that serves the dual purpose of X-ray detectors and momentum wheels. By employing passivity theory it is shown, that the satellite is a passive system. This paper shows, that global asymptotic stability can be obtained with a passive and an input and output strictly passive system in a feedback interconnection. It is demonstrated in a simulation study that the resultant controller has a potential for on-board implementation in the acquisition phase, where global stability of the control law is vital.

Keywords: Nonlinear attitude control, Passivity theory, Stability theory, Linear feedback

Nomenclature

The nomenclature used throughout this paper is listed in Table 1.

{I}	Earth Centred Celestial Coordinate Frame.
{B}	Body Axis Coordinate Frame.
{P}	Principal Axis Coordinate Frame.
{T}	Target Coordinate Frame.
{W}	Wheel Axis Coordinate Frame.
${}^{i}\boldsymbol{v}$, ${}^{b}\boldsymbol{v}$, ${}^{p}\boldsymbol{v}$, ${}^{w}\boldsymbol{v}$	Vector $\boldsymbol{v}$ resolved in the {I}-, {B}-, {P}-, or {W}-coordinate frame.
$A^{\dagger}$	The adjoint of A, i.e. $A^{\dagger} = (A^{\mathrm{T}})^{*}$.
A^{R}	Right pseudo-inverse of A.
${}^{b}_{w}A$	Transformation matrix: $\{W\} \mapsto \{B\}$.
${}^{p}_{b}A$	Transformation matrix: $\{B\} \mapsto \{P\}$.
$\boldsymbol{h}_w$	Angular momentum of WATCH.
$\mathcal{H}$	Operator performing the mapping, $\mathcal{H}\ :\ \boldsymbol{u}(t) \mapsto \boldsymbol{y}(t)$.
$I_{n\times n}$	A $n \times n$ identity matrix.
I_p	Principal inertia tensor of satellite.
I_w	Inertia tensor of WATCH instrument.
L	Angular momentum.
$\boldsymbol{N}_{dist}$	Environmental disturbance torque.
$\boldsymbol{N}_{ext}$	External torque.
$\boldsymbol{N}_w$	Control torque generated by WATCH.
$\boldsymbol{q}$, q_4	Vector and scalar part of unit attitude quaternion $\mathbf{q}$.
${}^{p}_{i}\mathbf{q}$	Attitude quaternion representing the orientation of {I} w.r.t. {P}.
${}^{i}_{t}\mathbf{q}$	Attitude quaternion representing the orientation of {T} w.r.t. {I}.
${}^{p}_{t}\mathbf{q}$	Attitude error quaternion.
$S(\boldsymbol{v})$	Skew-symmetric matrix of a vector $\boldsymbol{v}$: $$S(\boldsymbol{v}) = \begin{bmatrix} 0 & -v_3 & v_2 \\ v_3 & 0 & -v_1 \\ -v_2 & v_1 & 0 \end{bmatrix}.$$
$\boldsymbol{v}_s$	Stator voltage to the WATCH.
$V\big(\boldsymbol{x}(t)\big)$	Scalar Lyapunov candidate function.
$w\big(\boldsymbol{u}(t), \boldsymbol{y}(t)\big)$	Supply rate.
$\boldsymbol{x}_e$	Equilibrium point.
$\boldsymbol{v}_T(t)$	Truncated vector for $0 \leq t \leq T$.
$\boldsymbol{\omega}_{p,i}$	Angular velocity of {P} w.r.t. {I}.
$\boldsymbol{\omega}_w$	Angular velocity of WATCH.
$\Omega(\boldsymbol{v})$	Skew-symmetric matrix of a vector $\boldsymbol{v}$: $$\Omega(\boldsymbol{v}) = \begin{bmatrix} 0 & \boldsymbol{v}_3 & -\boldsymbol{v}_2 & \boldsymbol{v}_1 \\ -\boldsymbol{v}_3 & 0 & \boldsymbol{v}_1 & \boldsymbol{v}_2 \\ \boldsymbol{v}_2 & -\boldsymbol{v}_1 & 0 & \boldsymbol{v}_3 \\ -\boldsymbol{v}_1 & -\boldsymbol{v}_2 & -\boldsymbol{v}_3 & 0 \end{bmatrix}.$$

Table 1: Nomenclature.

I. Introduction

Typical actuators are: Momentum wheels, thrusters or electromagnetic coils. For the Danish Ørsted satellite[1] electromagnetic coils were employed as attitude actuators, since they are reliable, lightweight, and require low power. As a result of the success of the Ørsted satellite, the Danish Small Satellite Programme (DSSP) has chosen, that the Rømer satellite shall be the next Danish small satellite. To reduce costs and weight, it has been chosen to use WATCH (Wide Angle Telescopes for Cosmic Hard x-rays) telescopes, which perform rotary motion. The WATCH telescopes are placed in a tetrahedron configuration, which ensures total sky coverage. Attitude actuation using WATCH instruments is possible, since the scientific observations allow the instruments to have a varying angular frequency in the range: $\pm[0.5 - 2]Hz$.

Attitude control of the Rømer satellite, using WATCH instruments, is the topic of this paper. Because the satellite model is nonlinear, and global stability is required, passivity theory has been selected for the analysis and design of the Attitude Controller (AC). Passivity theory has a very physical and intuitive appeal.

The application of passivity and nonlinear control theory has proven to be feasible for the attitude control of satellites. As compared to linear control methods, nonlinear methods do not use model approximations. This means that global stability can be guaranteed, and that system behaviour is not restricted to a certain neighbourhood of a specific operating point.

Attitude control of satellites using passivity theory has been covered well in literature. Willems (1991) was the first to show, that a passive nonlinear system could be rendered globally asymptotically stable to an equilibrium point, by using pure gain output feedback.[2] Egeland and Godhavn (1994) derived an adaptive attitude controller for a rigid spacecraft, that was based on a linear parameterisation of the equation of motion.[3] The tracking error was described using Euler parameters. Passivity theory was then utilised to show global convergence of the tracking error to zero. A linear global asymptotic stabilising controller was derived by Tsiotras (1995), for the attitude motion of a rigid spacecraft.[4] This was done in terms of non-redundant kinematic parameters (Modified Rodrigues parameters). Using the inherent passivity property of the system it was shown, that the achieved results could be extended to stabilising control laws without angular velocity measurements. The rigid body stabilisation problem, without angular velocity measurements, was also treated by Lizarralde and Wen (1996).[5] A passivity approach was used to derive a wide class of filters for the error quaternion, which was used to replace the angular velocity in a standard PD-control law. Global asymptotic stability of the closed-loop system was shown using LaSalle's invariance principle. The derivation of a dynamic attitude controller for a spacecraft with flexible appendages was considered by Gennaro (1998).[6] The controller was able to perform slew manoeuvres, using only attitude measures. The passivity concept was used to ensure asymptotic convergence to the reference point.

The paper demonstrates, using the concepts of stability and non-linear system theory, that global asymptotic stability of a desired reference is achievable.

In this paper the attitude dynamics of the Rømer satellite and the WATCH dynamics will be modelled. By analysing the satellite's subsystems, it will be shown, that the satellite is a passive system. By using a memoryless state feedback, similar to the one obtained by Lizarralde[5], Dalsmo and Egeland[7], a feedback interconnection is obtained, capable of achieving global asymptotic stability of a reference operating point.

This paper is organised as follows. Section II considers passivity theory at large. In section III the Rømer satellite configuration, the modelling of the attitude dynamics, and the WATCH dynamics are described. By dividing the satellite attitude dynamics into dynamics and kinematics, it is shown that the satellite is a passive system. An AC with vector quaternion and angular velocity feedback is introduced. By having an AC which is input and output strictly passive it is shown, that the feedback interconnection renders the operating point global asymptotic stable. Control torque generation using the WATCH instruments is demonstrated. Finally, the principle of introducing the attitude reference is terms of an error quaternion is described. In section IV the results of a numerical simulation are presented. In section V the results are commented and discussed. Section VI presents the conclusions.

II. Passivity Theory

Some preliminaries of passivity theory used in this paper will be shortly reviewed for the consistency of the presentation.

Passivity is applied to non-linear systems which are modelled by ordinary differential equations with input vector $\boldsymbol{u}(t)$ and output vector $\boldsymbol{y}(t)$:

$$\mathcal{H} \begin{cases} \dot{\boldsymbol{x}}(t) = \boldsymbol{f}\big(\boldsymbol{x}(t), \boldsymbol{u}(t)\big) \\ \boldsymbol{y}(t) = \boldsymbol{h}\big(\boldsymbol{x}(t), \boldsymbol{u}(t)\big) \end{cases} \tag{1}$$

The system (1) is dissipative with the supply rate $w\big(\boldsymbol{u}(t), \boldsymbol{y}(t)\big)$ if it is not able to generate power by itself, that is the energy stored in the system is less than or equal to the supplied power[8]:

$$V\big(\boldsymbol{x}(t)\big) \geq 0 \text{ and} \tag{2}$$
$$V\big(\boldsymbol{x}(T)\big) - V\big(\boldsymbol{x}(0)\big) \leq \int_0^T w\big(\boldsymbol{u}(t), \boldsymbol{y}(t)\big)\, dt$$

Furthermore, the storage function $V\big(\boldsymbol{x}(t)\big)$ must satisfy the requirements for a Lyapunov function.

If there exist a positive semidefinite Lyapunov function, such that:

$$\begin{aligned} \boldsymbol{u}^{\mathrm{T}}(t)\, \boldsymbol{y}(t) \geq & \frac{\partial V\big(\boldsymbol{x}(t)\big)}{\partial \boldsymbol{x}(t)}\, \boldsymbol{f}\big(\boldsymbol{x}(t), \boldsymbol{u}(t)\big) \\ & + \epsilon \boldsymbol{u}^{\mathrm{T}}(t)\, \boldsymbol{u}(t) + \delta \boldsymbol{y}^{\mathrm{T}}(t)\, \boldsymbol{y}(t) \\ & + \rho \phi\big(\boldsymbol{x}(t)\big) \end{aligned} \tag{3}$$

then the system (1) is passive[8]. A passive system implies that any increase in storage energy is due solely to an external power supply.

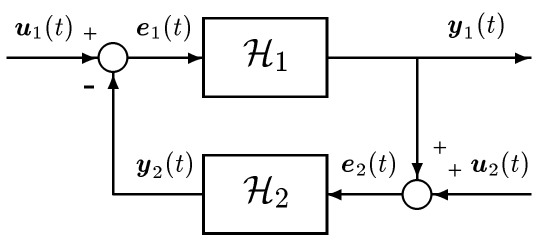

Fig. 1: Feedback interconnection of two passive systems.

Consider the feedback system in figure 1 with memoryless feedback and the dynamics of $\mathcal{H}_1$ as:

$$\begin{aligned} \dot{\boldsymbol{x}}_1(t) &= \boldsymbol{f}_1\big(\boldsymbol{x}_1(t),\, \boldsymbol{e}_1(t)\big) \\ \boldsymbol{y}_1(t) &= \boldsymbol{h}_1\big(\boldsymbol{x}_1(t),\, \boldsymbol{e}_1(t)\big) \end{aligned} \tag{4}$$

The system $\mathcal{H}_2$ is memoryless with the form:

$$\boldsymbol{y}_2(t) = \boldsymbol{h}_2\big(t,\, \boldsymbol{e}_2(t)\big) \tag{5}$$

If $\mathcal{H}_1$ is passive with a positive definite storage function $V_1\big(\boldsymbol{x}_1(t)\big)$ and $\mathcal{H}_2$ is just a passive system, that is:

$$\begin{aligned} \boldsymbol{e}_1^{\mathrm{T}}(t)\, \boldsymbol{y}_1(t) \geq & \frac{\partial V_1\big(\boldsymbol{x}_1(t)\big)}{\boldsymbol{x}_1(t)} \boldsymbol{f}_1\big(\boldsymbol{x}_1(t),\, \boldsymbol{e}_1(t)\big) \\ & + \epsilon_1 \boldsymbol{e}_1^{\mathrm{T}}(t)\, e_1(t) + \delta_1 \boldsymbol{y}_1^{\mathrm{T}}(t)\, \boldsymbol{y}_1(t) \\ & + \rho_1 \psi_1\big(\boldsymbol{x}_1(t)\big) \\ \boldsymbol{e}_2^{\mathrm{T}}(t)\, \boldsymbol{y}_2(t) \geq & \, \epsilon_2 \boldsymbol{e}_2^{\mathrm{T}}(t)\, \boldsymbol{e}_2(t) + \delta_2 \boldsymbol{y}_2^{\mathrm{T}}(t)\, \boldsymbol{y}_2(t) \end{aligned} \tag{6}$$

Then the equilibrium point of:

$$\dot{\boldsymbol{x}}(t) = \boldsymbol{f}\big(t,\, \boldsymbol{x}(t),\, \boldsymbol{0}\big) \tag{7}$$

is uniformly stable[8]. If $\mathcal{H}_2$ is time invariant, then the equilibrium point in of the system in (7) is asymptotically stable in either of the two cases:

1. $\rho_1 > 0$.
2. $\epsilon_2 + \delta_1 > 0$ and $\mathcal{H}_1$ is zero-state observable.

The origin will be globally asymptotically stable if $V_1\big(\boldsymbol{x}_1(t)\big)$ is radially unbounded[8].

III. The Rømer Satellite

This section describes the configuration of the Rømer satellite, the satellite modelling, the passivity analysis of the satellite model, and the design of a passivity based attitude controller capable of providing global asymptotic stability to a desired reference. Subsequently, control torque generation using the WATCH instruments is described.

Satellite Configuration

The Rømer satellite, which is planned to be launched in year 2003, will carry two scientific experiments called the MONS (Measuring Oscillations in Nearby Stars) and the Ballerina experiment. The two experiments were suggested as two separate satellite missions. Due to the great overlap between them it was decided to combine the to missions in one satellite - the Rømer satellite.

The instrumentation of the Rømer satellite must consequently satisfy the scientific objectives of the two missions - a challenging task since the satellite must be very compact in order to be launched as a secondary payload. The orbit specified for the Rømer satellite is a Molniya orbit, named after the orbit used by Russian communication satellites.

The scientific objective of MONS is to strengthen substantially the fundamental basis of astrophysics which stellar astrophysics provides. This will be accomplished by carrying out observation of stellar oscillations at a greatly improved level of sensitivity. A typical target is going to be observed for 30-50 days continuously. This is performed to probe the stellar interior for determination of its composition, age, and internal rotation. The primary instrument specified on the MONS mission is a $340mm$ telescope with a CCD (Charged Coupled Device) detector.

The scientific objective of Ballerina is the detection and localisation of GRBs (gamma-ray bursts). The physical mechanism leading to GRBs is poorly understood. Gamma-ray bursts occur randomly and are distributed over the entire sky, and are known to be among the farthest objects in the universe. The scientific instrument specified for the Ballerina mission is an $80mm$ X-ray telescope.

After a GRB has been detected, by one of the WATCH instruments, and localised at a precision of approximately 1 arc minute, the satellite turns autonomously within a few minutes to allow the X-ray telescope to observe the following afterglow. The star imager and the X-ray telescope then determine the precise source of the burst. Subsequently, results are transmitted to the Earth, to allow more advanced ground telescopes as well as space-based telescopes, to perform more detailed observations. The spectral and time evolution of the fading afterglow source is observed until it is to faint.

In the observation mode the requirement for the pointing accuracy is 30 arc seconds RMS on all axes.

The WATCH instruments are organised in a tetrahedron configuration, i.e. an angle of $109.47°$ exists between any two instrument axes. The tetrahedron configuration offers redundancy in that the attitude can still be controlled if one of the instruments fails.

The instrumentation of the Rømer satellite is shown in Fig. 2.

Satellite Modelling

The four WATCH instruments serve both a scientific and a control purpose.

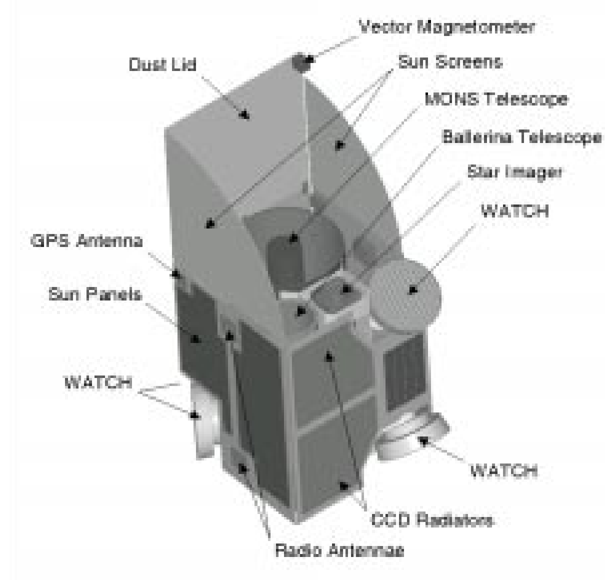

Fig. 2: Proposed layout of the Rømer satellite - satellite dimensions: $600 \times 600 \times 800mm$ (W×D×H), and weight: $120kg$.

The WATCH instruments generate the angular momentum ${}^p\boldsymbol{h}_w$, which is found by adding the angular momenta generated along the individual wheel axes. The angular momentum of one WATCH instrument in the {W} coordinate frame is given by *:

$$\begin{aligned} {}^w\dot{h}_w(t) &= K_t\left(\frac{{}^w v_s - K_e\,{}^w\omega_w}{R_s}\right) - B_v\,{}^w\omega_w \\ &= -\left(\frac{K_t\,K_e + B_v\,R_s}{R_s}\right){}^w\omega_w + \frac{K_t}{R_s}\,{}^w v_s \\ &= -A_w\,{}^w\omega_w + B_w\,{}^w v_s \end{aligned} \tag{8}$$

where the coulomb friction has been omitted. The rate of change of the total angular momentum of the satellite[10], given in the Principal Axis Coordinate Frame, is described by:

$$\begin{aligned} I_p\,{}^p\dot{\boldsymbol{\omega}}_{p,i}(t) = &-S\left({}^p\boldsymbol{\omega}_{p,i}(t)\right)\,I_p\,{}^p\boldsymbol{\omega}_{p,i}(t) \\ &-S\left({}^p\boldsymbol{\omega}_{p,i}(t)\right)\,{}^p\boldsymbol{h}_w(t) \\ &-\underbrace{{}^p\boldsymbol{N}_w(t)}_{{}^p_wA\,{}^w\dot{\boldsymbol{h}}_w(t)} + {}^p\boldsymbol{N}_{dist}(t) \end{aligned} \tag{9}$$

The external torque ${}^p\boldsymbol{N}_{ext}$ exists due to the presence of environmental disturbance torques acting on the satellite.

For representation of the attitude the unit quaternion has been chosen. The quaternion attitude

*Standard dynamic model of a DC motor.[9]

representation is convenient since only four parameters are needed to represent the attitude globally, compared to the nine parameters used in a direction cosine transformation matrix. The rate of change of the attitude quaternion ${}^{p}_{i}\mathbf{q}$ is given by:

$$\frac{d}{dt}\,{}^{p}_{i}\mathbf{q} = \frac{1}{2}\Omega\left({}^{p}\boldsymbol{\omega}_{p,i}\right)\,{}^{p}_{i}\mathbf{q} \tag{10}$$

where the skew-symmetric matrix $\Omega\left({}^{p}\boldsymbol{\omega}_{p,i}\right)$ is formed on the basis of the satellite's instantaneous angular velocity vector ${}^{p}\boldsymbol{\omega}_{p,i}$ (see the nomenclature in Table 1).

Passivity Analysis of the Satellite

The purpose of this section is to check whether or not the satellite is a passive system. For this purpose the satellite model is divided into several subsystems (see Fig. 3), which are analysed separately. These mappings will be analysed with respect to their passivity properties: The mapping of the WATCH instrument: ${}^{w}v_s \mapsto {}^{w}\omega_w$, the mapping of the dynamics: $[{}^{p}\boldsymbol{h}_w,\, {}^{p}\boldsymbol{N}_w]^{\mathrm{T}} \mapsto {}^{p}\boldsymbol{\omega}_{p,i}$, and finally the kinematic mapping: ${}^{p}\boldsymbol{\omega}_{p,i} \mapsto {}^{p}_{i}\boldsymbol{q}$.

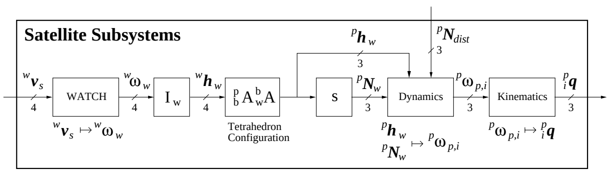

Fig. 3: Satellite subsystems and mappings between inputs and outputs.

The tetrahedron transformation from {W} to {P} will not be analysed, since it only describes the orientation of the WATCH instruments. The inertia matrix of the WATCH instrument I_w will not be analysed since a positive definite matrix can be shown to be input and output strictly passive. The differentiator is also passive, since the storage function $V\left(\boldsymbol{x}(t)\right) = \frac{1}{2}\boldsymbol{x}^{\mathrm{T}}(t)\,\boldsymbol{x}(t)$ has a time derivative equal to $\dot{V}\left(\boldsymbol{x}(t)\right) = \boldsymbol{x}^{\mathrm{T}}(t)\,\dot{\boldsymbol{x}}(t) = \boldsymbol{u}^{\mathrm{T}}(t)\,\boldsymbol{y}(t)$.

The storage function of a rotating wheel is given by its kinetic energy: $V({}^{w}\omega_w) = \frac{1}{2}I_w\,{}^{w}\omega_w{}^2$. The change in energy storage is given by its time derivative:

$$\dot{V}({}^{w}\omega_w) = {}^{w}\omega_w\,I_w\,{}^{w}\dot{\omega}_w \tag{11}$$

Inserting the dynamic model of the i'th WATCH instrument from Eq. 8 into Eq. 11, it becomes possible to isolate the power flow $y\,u = {}^{w}\omega_w\,{}^{w}v_s$:

$$\begin{aligned} {}^{w}\omega_w\,{}^{w}v_s &= \frac{1}{B_w}\,\dot{V}({}^{w}\omega_w) + \frac{A_w}{B_w}\,{}^{w}\omega_w{}^2 \\ &\geq \dot{V}({}^{w}\omega_w)\;,\;\; A_w > 0\;,\;\; 0 < B_w < 1 \end{aligned} \tag{12}$$

where $B_w = \frac{K_t}{R_s} < 1$. Consequently, it can be concluded, that the WATCH instrument performs a passive mapping.

If it can be shown, that the mapping ${}^{p}\boldsymbol{N}_w \mapsto {}^{p}\boldsymbol{\omega}_{p,i}$ is passive, then the mapping ${}^{p}\boldsymbol{h}_w \mapsto {}^{p}\boldsymbol{\omega}_{p,i}$ will also be passive, since a differentiator is a passive system as shown previously.

The passivity analysis of the satellite dynamics is performed by calculating the inner product between the input and output of the mapping ${}^{p}\boldsymbol{N}_w \mapsto {}^{p}\boldsymbol{\omega}_{p,i}$:

$$\langle {}^{p}\boldsymbol{\omega}_{p,i}, {}^{p}\boldsymbol{N}_w\rangle_T = \int_0^T {}^{p}\boldsymbol{\omega}_{p,i}{}^{\mathrm{T}}(t)\,{}^{p}\boldsymbol{N}_w(t)\;dt \tag{13}$$

Inserting Eq. 9 into Eq. 13, and neglecting the disturbance torque, it can be concluded, that the satellite dynamics performs a passive mapping:

$$\begin{aligned} &\langle {}^{p}\boldsymbol{\omega}_{p,i}, {}^{p}\boldsymbol{N}_w\rangle_T = \\ &\quad -\int_0^T {}^{p}\boldsymbol{\omega}_{p,i}{}^{\mathrm{T}}(t)\,I_p\,{}^{p}\dot{\boldsymbol{\omega}}_{p,i}(t)\;dt \\ &\quad -\int_0^T {}^{p}\boldsymbol{\omega}_{p,i}{}^{\mathrm{T}}(t)\;S\left({}^{p}\boldsymbol{\omega}_{p,i}(t)\right)\,I_p\,{}^{p}\boldsymbol{\omega}_{p,i}(t)\;dt \\ &\quad -\int_0^T {}^{p}\boldsymbol{\omega}_{p,i}{}^{\mathrm{T}}(t)\;S\left({}^{p}\boldsymbol{\omega}_{p,i}(t)\right){}^{p}\boldsymbol{h}_w(t)\;dt \\ &= -\int_{{}^{p}\boldsymbol{\omega}_{p,i}(0)}^{{}^{p}\boldsymbol{\omega}_{p,i}(T)} {}^{p}\boldsymbol{\omega}_{p,i}{}^{\mathrm{T}}(t)\,I_p\,d\,{}^{p}\boldsymbol{\omega}_{p,i} \\ &= -\frac{1}{2}\Big[{}^{p}\boldsymbol{\omega}_{p,i}{}^{\mathrm{T}}(T)\,I_p\,{}^{p}\boldsymbol{\omega}_{p,i}(T) \\ &\qquad\quad - {}^{p}\boldsymbol{\omega}_{p,i}{}^{\mathrm{T}}(0)\,I_p\,{}^{p}\boldsymbol{\omega}_{p,i}(0)\Big] \\ &= -\Big[V\left({}^{p}\boldsymbol{\omega}_{p,i}(T)\right) - V\left({}^{p}\boldsymbol{\omega}_{p,i}(0)\right)\Big] \\ &= \beta \end{aligned} \tag{14}$$

where β is some finite value, since the angular velocities have been truncated, and ${}^{p}\boldsymbol{\omega}_{p,i}{}^{\mathrm{T}}(t)\;S\left({}^{p}\boldsymbol{\omega}_{p,i}(t)\right) = \mathbf{0}^{\mathrm{T}}$. It can be seen, that a positive work performed on the dynamics is equal to a positive change in kinetic energy $V({}^{p}\boldsymbol{\omega}_{p,i}) = \frac{1}{2}{}^{p}\boldsymbol{\omega}_{p,i}I_p{}^{p}\boldsymbol{\omega}_{p,i}$. The minus sign in

Eq. 14 is due to the fact, that the control torque is generated internally.

In order to check passivity of the mapping ${}^{p}\boldsymbol{\omega}_{p,i} \mapsto {}^{p}_{i}\boldsymbol{q}$ the inner product between the input and output is calculated:

$$\langle {}^{p}_{i}\boldsymbol{q}, {}^{p}\boldsymbol{\omega}_{p,i} \rangle_T = \int_0^T {}^{p}_{i}\boldsymbol{q}^{\mathrm{T}}(t)\ {}^{p}\boldsymbol{\omega}_{p,i}(t)\ dt \qquad (15)$$

From Eq. 10 it can be found, that ${}^{p}_{i}\dot{q}_4(t) = -\frac{1}{2}\ {}^{p}_{i}\boldsymbol{q}^{\mathrm{T}}(t)\ {}^{p}\boldsymbol{\omega}_{p,i}(t)$. When inserted into Eq. 15 the following is obtained:

$$\begin{aligned} \langle {}^{p}_{i}\boldsymbol{q}, {}^{p}\boldsymbol{\omega}_{p,i} \rangle_T &= -2\int_0^T {}^{p}_{i}\dot{q}_4(t)\ dt \qquad (16) \\ &= -2\int_{{}^{p}_{i}q_4(0)}^{{}^{p}_{i}q_4(T)} d\,{}^{p}_{i}q_4 \\ &= 2\left[{}^{p}_{i}q_4(0) - {}^{p}_{i}q_4(T)\right] \end{aligned}$$

Because ${}^{p}_{i}q_4 \equiv \cos\frac{\Phi}{2}$ is bounded by $|{}^{p}_{i}q_4(t)| \leq 1$ for all t, the bracket $\left[{}^{p}_{i}q_4(0) - {}^{p}_{i}q_4(T)\right]$ is bounded by $\left|{}^{p}_{i}q_4(0) - {}^{p}_{i}q_4(T)\right| \leq 2$. Therefore Eq. 16 can be written as:

$$\langle {}^{p}_{i}\boldsymbol{q}, {}^{p}\boldsymbol{\omega}_{p,i} \rangle_T \geq -4 = \beta \qquad (17)$$

Since the inner product is lower bounded by a constant $\beta = -4$, it can be concluded, that the mapping ${}^{p}\boldsymbol{\omega}_{p,i} \mapsto {}^{p}_{i}\boldsymbol{q}$ is passive. The exact same result was obtained by Egeland and Godhavn.[3]

We have not been able to prove mathematically, that a series connection of two passive systems results in an interconnection which is also passive. A satellite, however, is known to be a conservative system, and consequently, it has no internal power production. A system like this is passive.

Control Law Design

Having a satellite which is passive, it is possible to render the satellite globally asymptotically stable to a reference attitude by using a memoryless feedback, i.e. a feedback which is input and output strictly passive.

By choosing the feedback wheel torque ${}^{p}\boldsymbol{N}_w$ as:

$${}^{p}\boldsymbol{N}_w = k_p\,{}^{p}_{i}\boldsymbol{q} + k_d\,{}^{p}\boldsymbol{\omega}_{p,i}\ ,\quad k_p,\ k_d > 0 \qquad (18)$$

a memoryless feedback is achieved which is input and output strictly passive. This is demonstrated in the following.

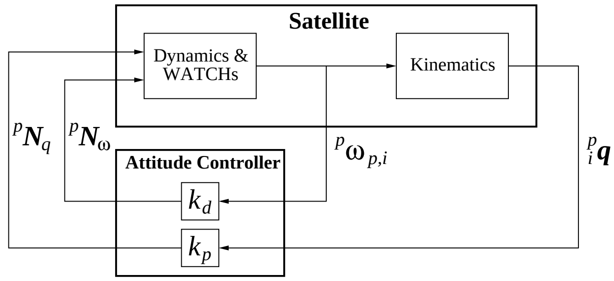

Fig. 4: Attitude Control System comprised of the satellite and the Attitude Controller.

The interconnection of the attitude controller and the satellite is sketched in Fig. 4. By writing the controller's output vector ${}^{p}\boldsymbol{N}_w$ in Eq. 18 as: ${}^{p}\boldsymbol{N}_w = {}^{p}\boldsymbol{N}_\omega + {}^{p}\boldsymbol{N}_q$, it is possible to analyse the passivity properties of the mapping: $[{}^{p}\boldsymbol{\omega}_{p,i}\ ,\ {}^{p}_{i}\boldsymbol{q}]^{\mathrm{T}} \mapsto [{}^{p}\boldsymbol{N}_\omega\ ,\ {}^{p}\boldsymbol{N}_q]^{\mathrm{T}}$ sketched in Fig. 5. The reason is, that the passivity analysis (the calculation of the inner-product) requires, that the input and output vector are of same dimension. The

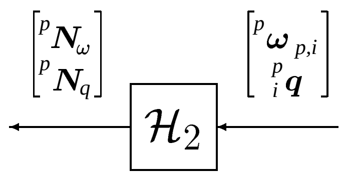

Fig. 5: Control law from Eq. 18.

controller performs the following mapping:

$$\underbrace{\begin{bmatrix} {}^{p}\boldsymbol{N}_\omega \\ {}^{p}\boldsymbol{N}_q \end{bmatrix}}_{\boldsymbol{y}} = \underbrace{\begin{bmatrix} k_d\, I_{3\times 3} & 0 \\ 0 & k_p\, I_{3\times 3} \end{bmatrix}}_{\mathcal{H}_2} \underbrace{\begin{bmatrix} {}^{p}\boldsymbol{\omega}_{p,i} \\ {}^{p}_{i}\boldsymbol{q} \end{bmatrix}}_{\boldsymbol{u}} \qquad (19)$$

where $k_p,\ k_d > 0$. The matrix $\mathcal{H}_2 : \mathbb{R}^6 \mapsto \mathbb{R}^6$ has been chosen such, that $\mathcal{H}_2^{-1}$ exists, and $\mathcal{H}_2$ becomes diagonal.

The power flow $\boldsymbol{y}^{\mathrm{T}}\,\boldsymbol{u} = \boldsymbol{u}^{\mathrm{T}}\,\boldsymbol{y}$ into the system is:

$$\boldsymbol{y}^{\mathrm{T}}\,\boldsymbol{u} = \boldsymbol{u}^{\mathrm{T}}\,\mathcal{H}_2^{\mathrm{T}}\,\boldsymbol{u} = \boldsymbol{y}^{\mathrm{T}}\,\mathcal{H}_2^{-1}\,\boldsymbol{y} \qquad (20)$$

Note that $\boldsymbol{y}^{\mathrm{T}}\,\boldsymbol{u}$ is equivalent to:

$$\boldsymbol{y}^{\mathrm{T}}\,\boldsymbol{u} = \frac{1}{2}\left(\boldsymbol{u}^{\mathrm{T}}\,\mathcal{H}_2^{\mathrm{T}}\,\boldsymbol{u}\right) + \frac{1}{2}\left(\boldsymbol{y}^{\mathrm{T}}\,\mathcal{H}_2^{-1}\,\boldsymbol{y}\right) \geq 0 \qquad (21)$$

The power flow $\boldsymbol{y}^{\mathrm{T}}\,\boldsymbol{u}$ is always nonnegative, since both $\mathcal{H}_2^{\mathrm{T}}$ and $\mathcal{H}_2^{-1}$ will have positive eigenvalues, due to the structure of $\mathcal{H}_2$. Eq. 21 states, that the controller is input and output strictly passive, since both ϵ_2 and δ_2 are positive constants.

If either k_d or k_p, or both are zero the controller will not be input and output strictly passive, since then $\mathcal{H}_2^{-1}$ will not exists. If either k_d or k_p, or both are negative, ϵ_2 and δ_2 cannot be guaranteed to be positive for every input and output.

If it can be shown, that the satellite model with the passive mapping $\mathcal{H}_1$ is ZSO, the equilibrium point will be asymptotically stable:

$$\epsilon_2 + \delta_1 > 0 \ , \quad \text{and } \mathcal{H}_1 \text{ ZSO}$$

First of all $\mathcal{H}_2$ must be time invariant. This is also the case. Since $\epsilon_2 > 0$ and $\delta_1 = 0$, it only needs to be shown, that the satellite is ZSO. This requires, that only the trivial solution $\boldsymbol{x}_e$ of Eq. 9 can stay identically in $\mathbb{S} = \{\boldsymbol{x}(t) \in \mathbb{R}^n \,|\, \boldsymbol{y}(t) = \boldsymbol{h}(\boldsymbol{x}(t), \boldsymbol{0}) = \boldsymbol{0}\}$. This is the case for the satellite model, since the output is in fact the states of the system, i.e. zero output, with zero input, will in all future result in the states being equal to zero.

Finally, since the following Lyapunov candidate function

$$\begin{aligned} V\left({}^p_i q_4, {}^p\boldsymbol{\omega}_{p,i}\right) &= 2\,k_p\,\left(1 - {}^p_i q_4\right) \\ &\quad + \frac{1}{2}\,{}^p\boldsymbol{\omega}_{p,i}{}^{\mathrm{T}}\,I_p\,{}^p\boldsymbol{\omega}_{p,i} \ , \quad k_p > 0 \end{aligned} \tag{22}$$

is radially unbounded the equilibrium point $\boldsymbol{x}_e = \left[{}^p\boldsymbol{\omega}_{p,i_e} \, , \, {}^p_i\boldsymbol{q}_e\right]^{\mathrm{T}} = \boldsymbol{0}$ is globally asymptotically stable.

Torque Generation using WATCH Instruments

When transforming the torque vector ${}^w\boldsymbol{N}_w$ to the Principle Axis Coordinate Frame by ${}^p_wA = {}^p_bA\,{}^b_wA$, the following is obtained:

$$\begin{aligned} {}^p\boldsymbol{N}_w &= {}^p_wA\,{}^w\boldsymbol{N}_w = {}^p_wA\,A_w\,I_{4\times4}\,{}^w\boldsymbol{\omega}_w \\ &\quad - {}^p_wA\,B_c\,I_{4\times4}\,\mathrm{sign}({}^w\boldsymbol{\omega}_w) \\ &\quad + {}^p_wA\,B_w\,I_{4\times4}\,{}^w\boldsymbol{v}_s \end{aligned} \tag{23}$$

Due to the tetrahedron configuration of the WATCH instruments, the transformation matrix ${}^b_wA$ is a 3×4 matrix given by:

$$\begin{aligned} {}^b_wA &= \begin{bmatrix} {}^b\hat{\boldsymbol{w}}_1 & {}^b\hat{\boldsymbol{w}}_2 & {}^b\hat{\boldsymbol{w}}_3 & {}^b\hat{\boldsymbol{w}}_4 \end{bmatrix} \\ &= \begin{bmatrix} -0.817 & 0.817 & 0 & 0 \\ -0.577 & -0.577 & 0.577 & 0.577 \\ 0 & 0 & -0.817 & 0.817 \end{bmatrix} \end{aligned} \tag{24}$$

and the direction cosine transformation matrix ${}^b_pA$ is given by:

$$\begin{aligned} {}^b_pA &= \begin{bmatrix} {}^b\boldsymbol{p}_x & {}^b\boldsymbol{p}_y & {}^b\boldsymbol{p}_z \end{bmatrix} \\ &= \begin{bmatrix} 0.23 & -0.97 & 0.01 \\ 0.92 & 0.22 & 0.33 \\ -0.32 & -0.07 & 0.95 \end{bmatrix} \end{aligned} \tag{25}$$

Solving Eq. 23 with respect to the control voltage vector ${}^w\boldsymbol{v}_s$ yields:

$$\begin{aligned} {}^w\boldsymbol{v}_s = B_w{}^{-1}\,{}^p_wA^{\mathrm{R}}\Big[\,&{}^p\boldsymbol{N}_w \\ &- {}^p_wA\,A_w\,I_{4\times4}\,{}^w\boldsymbol{\omega}_w \\ &+ {}^p_wA\,B_c\,I_{4\times4}\,\mathrm{sign}({}^w\boldsymbol{\omega}_w)\Big] \end{aligned} \tag{26}$$

where the 4×3 matrix ${}^p_wA^{\mathrm{R}}$ is the right pseudo-inverse† of the 3×4 transformation matrix ${}^p_wA$, which describes the orientation of the WATCH instruments within the tetrahedron configuration.

The least squares solution, that minimises $\|\boldsymbol{x}\|$ in the following equation:

$$A_{n\times m}\boldsymbol{x}_{m\times1} = \boldsymbol{y}_{n\times1} \ , \quad m > n \tag{27}$$

is given by finding the right pseudo-inverse of $A_{n\times m}$.[11] Consequently, ${}^p_wA^{\mathrm{R}}$ is given by:

$${}^p_wA^{\mathrm{R}} = {}^p_wA^{\dagger}\left({}^p_wA\,{}^p_wA^{\dagger}\right)^{-1} \tag{28}$$

Based on Eq. 26 it is possible to sketch the structure of the AC (see Fig. 6).

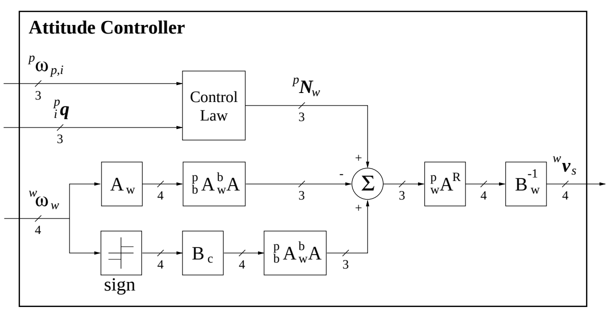

Fig. 6: Block diagram of the Attitude Controller structure.

Introducing the Attitude Reference

In order to make the AC track references the use of an error quaternion is suggested.[10] The principle is based on a transformation of the satellite's

†Also referred to as the Moore-Penrose generalised matrix inverse.

attitude quaternion ${}^{p}_{i}\mathbf{q}$. The principle is sketched in Fig. 7.

The idea is, that a desired target attitude is formulated by a target quaternion ${}^{t}_{i}\mathbf{q}$, which describes the orientation of the Earth Centred Celestial Coordinate Frame {I} with respect to the Target Coordinate Frame {T}. The purpose of the AC is to minimise changes in the attitude quaternion. By feeding back the error quaternion ${}^{p}_{t}\mathbf{q}$ instead of the actual attitude quaternion ${}^{p}_{i}\mathbf{q}$ the controller will initiate the necessary actions in order to realign the Principal Axis Coordinate Frame with the specified Target Coordinate Frame.

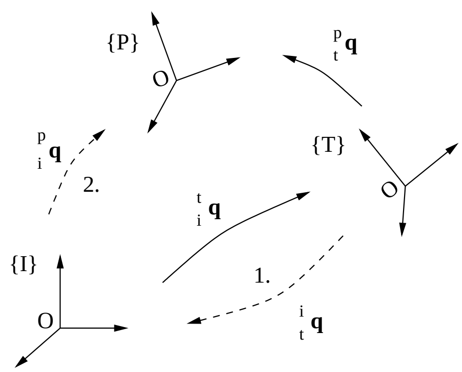

Fig. 7: Transformations used in calculating the error quaternion ${}^{p}_{t}\mathbf{q}$.

The error quaternion ${}^{p}_{t}\mathbf{q}$ is calculated as the error in rotation between the {T} and the {P} frames. Since both the orientation of the {P} and the {T} coordinate frame is known in terms of their orientation with respect to the {I} coordinate frame, the error quaternion can be calculated as sketched in Fig. 7. The path from {T} to {P} is given in two steps:

1. Perform the transformation from {T} to {I} given by the inverse of the reference quaternion, i.e. ${}^{i}_{t}\mathbf{q}$.
2. Transform ${}^{i}_{t}\mathbf{q}$ with the transformation from {I} to {P} given by the satellite's attitude quaternion ${}^{p}_{i}\mathbf{q}$.

Using quaternion multiplication[10] the error quaternion ${}^{p}_{t}\mathbf{q}$ is given by:

$${}^{p}_{t}\mathbf{q} = {}^{i}_{t}\mathbf{q}\,{}^{p}_{i}\mathbf{q} = \begin{bmatrix} {}^{p}_{i}q_4 & {}^{p}_{i}q_3 & -{}^{p}_{i}q_2 & {}^{p}_{i}q_1 \\ -{}^{p}_{i}q_3 & {}^{p}_{i}q_4 & {}^{p}_{i}q_1 & {}^{p}_{i}q_2 \\ {}^{p}_{i}q_2 & -{}^{p}_{i}q_1 & {}^{p}_{i}q_4 & {}^{p}_{i}q_3 \\ -{}^{p}_{i}q_1 & -{}^{p}_{i}q_2 & -{}^{p}_{i}q_3 & {}^{p}_{i}q_4 \end{bmatrix} \begin{bmatrix} {}^{i}_{t}q_1 \\ {}^{i}_{t}q_2 \\ {}^{i}_{t}q_3 \\ {}^{i}_{t}q_4 \end{bmatrix} \tag{29}$$

IV. Numerical Simulation Results

In this section the control law in Eq. 18 will be tested by means of a numerical simulation.

The satellite is a rigid body with the inertia tensor:

$$I_p \approx \begin{bmatrix} 8.3 & 0 & 0 \\ 0 & 6.6 & 0 \\ 0 & 0 & 4.0 \end{bmatrix} kgm^2 \tag{30}$$

The satellite is subject to zero initial angular velocity and the initial orientation is given by the attitude quaternion ${}^{p}_{i}\mathbf{q}(0)$:

$${}^{p}_{i}\mathbf{q}(0) = [0.462,\ 0.462,\ 0.653,\ 0.383]^{\mathrm{T}} \tag{31}$$

The environmental disturbance torque is modelled for the Molniya orbit, and includes the solar radiation, the gravity gradient, and the aerodynamic drag.

It has been chosen to use the following values for k_p and k_d:

- The proportional gain: $k_p = 0.5$.
- The differential gain: $k_d = 2.5$.

No quantisations have been introduced in order to keep the results as clear as possible. The attitude reference was set to: ${}^{t}_{i}\mathbf{q} = [0, 0, 0, 1]^{\mathrm{T}}$, in order to perform a slew manoeuvre.

The simulation results are shown in Fig. 8. The simulation is started at perigee, and it can be seen, that the environmental disturbance torque (2nd plot) forces the frequencies of the WATCH instruments (1st plot) to accelerate in order to bring the attitude error (3th plot) to zero.

V. Discussion of Results

The satellite was confirmed to be a passive system and a control law was designed capable of achieving global asymptotic stability of a reference point.

Torque control of the WATCH instruments was made possible by distributing the required control torque among the four WATCH instruments, using a right pseudo inverse matrix, i.e. an optimal way of solving four equations in three unknowns has been chosen, which minimises the solution (in this case the control voltage).

Using the concept of an attitude error quaternion the ACS was capable of performing reference tracking using quaternions.

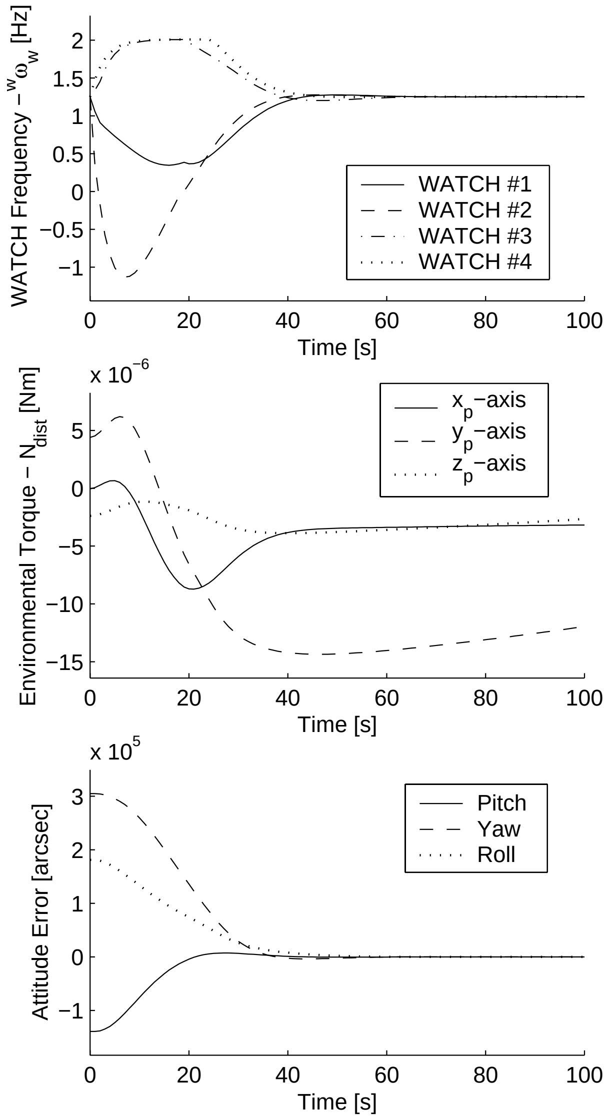

Fig. 8: Numerical simulation results.

As the test results showed, the AC is capable of stabilising the satellite, even at the perigee passage, to an accuracy well below the required 30 arc seconds RMS on all axes. If zoomed the result will be in the range ± 3 arc seconds. It is also evident from the attitude error plot, that the AC is capable of performing slew manoeuvres. Detailed slew manoeuvre tests have showed, that a rotation of $180°$ can be performed within approximately 150 seconds, i.e. a slew-rate of $1.2°/s$ can be obtained.[12]

VI. Conclusion

The purpose of this paper has been to present the results obtained through our master's work. The main result was the development of a linear feedback control law capable of achieving global asymptotic stability of the operating point.

In this paper we have tried to present the theory of passive systems in a way, that gives a clear overview of this wide topic. The presentation was mainly based on Sepulchre[8] and Khalil[13].

We did not succeed in showing mathematically, that a series connection of two or more passive systems is again a passive system.

The test results showed, that the pointing stability requirements for the Rømer satellite could be met even at perigee where the environmental disturbance are relatively large compared to the disturbances encountered at apogee. Simulation results have showed, that angular momentum dumping of the WATCH instruments, using for example electromagnetic coils, must be initiated after a maximum of 6 orbits (each orbit takes approximately 12 hours).[12]

Acknowledgement

The work was supported in part by the Danish Research Agency under the project Advanced Control Concepts for Precision Pointing of Small Spacecrafts.

References

1 Wis̆niewski, R. and Blanke, M. 1999, *Fully magnetic attitude control for spacecraft subject to gravity gradient*, Pergamon Press, Automatica 35, pp. 1201-1214.

2 Willems, J. C. and Isidori, A. 1991, *Passivity, feedback equivalence, and global stabilization of minimum phase systems*, IEEE Transactions on Automatic Control, Vol. 36, No. 11, pp. 1228-1240.

3 Egeland, O. and Godhavn, J.-M. April, 1994, *Passivity-Based Adaptive Attitude Control of a Rigid Spacecraft*, IEEE Transactions on Automatic Control, Vol. 39, No. 4, pp. 842-846.

4 Tsiotras, P. December, 1995, *A Passivity Approach to Attitude Stabilisation Using Nonredundant Kinematic Parameterisation*, 34th IEEE Conference on Decision & Control, New Orleans, LA, USA, pp. 515-520.

5 Lizarralde, F. and Wen, J. T. March, 1996, *Attitude Control Without Angular Velocity Measurement: A Passivity Approach*, IEEE Transactions on Decision & Control, Vol. 41, No. 3, pp. 468-472.

6 Gennaro, S. D. December, 1998, *Output Attitude Control of Flexible Spacecraft from Quaternion*

Measures: a Passivity Approch, 37th IEEE Conference on Decision & Control, Tampa, Florida USA, pp. 4549-.

[7] Dalsmo, M. and Egeland, O. August, 1997, *State Feedback $\mathcal{H}_\infty$-Suboptimal Control of a Rigid Spacecraft*, IEEE Transactions on Automatic Control, Vol. 42, No. 8, pp. 1186-1189.

[8] Sepulchre, R. and Jankoviĉ, R. 1997, *Constructive Nonlinear Control*, Springer-Verlag.

[9] Franklin, G. F. and Powell, J. D. 1994, *Feedback Control of Dynamic Systems*, Addison-Wesley Publishing Company, Inc., third edn.

[10] Wertz, J. R., editor 1997, *Spacecraft Attitude Determination and Control*, Kluwer Academic Publishers.

[11] Doyle, J. C. and Glover, K. 1996, *Robust and Optimal Control*, Prentice-Hall, Inc.

[12] Krogh-Sørensen, J. and Quottrup, M. M. June, 2000, *Passivity Based Nonlinear Attitude Control - of the Rømer Satellite*, Master's Thesis, Institute of Electronic Systems, Aalborg University.

[13] Khalil, H. K. 1996, *Nonlinear Systems*, Prentice-Hall, Inc., second edn.